



ELSEVIER

Contents lists available at ScienceDirect

Ad Hoc Networks

journal homepage: www.elsevier.com/locate/adhoc

Distributed audio sensing with homeostasis-inspired autonomous communication

Baris Atakan, Ozgur B. Akan*

Department of Electrical and Electronics Engineering, Koc University, 34450 Istanbul, Turkey

ARTICLE INFO

Article history:

Available online xxx

Keywords:

Wireless multimedia sensor networks
Bio-inspired networking
Audio sensing
Autonomous communication

ABSTRACT

Emerging applications of wireless sensor networks (WSN) requiring wide-band event signal communication such as multimedia surveillance sensor networks impose additional challenges including high communication bandwidth requirement and energy cost. Besides their partially or fully dependency on feedback messages from sink node, the existing protocols designed for WSN do not address the communication of wide-band event signals. Furthermore, the feedback messages may not reach in time to provide reliable communication of event information and save scarce network resources. Therefore, an autonomous communication protocol is imperative in order to provide wide-band event signal communication without any feedback from the sink. In nature, biological systems have self-organization capability, i.e., *homeostasis*, as they autonomously maintain a relatively stable equilibrium state for operation of vital functions. Hence, this natural phenomenon clearly gives promising inspirations in order to develop autonomous and efficient communication models and protocols for WSN domain. In this paper, the homeostasis-inspired autonomous communication (HAC) protocol is introduced for wireless audio sensor networks (WASN). Using the spectral properties of the wide-band event signal, i.e., audio signal, HAC enables WASN to maintain a relatively stable state in which sensor nodes reliably and energy-efficiently communicate the event signal to the sink node. Furthermore, with its self-organization capability, HAC does not rely on any feedback message from the sink node. Performance evaluations reveal that HAC successfully communicates wide-band event signal with minimum energy expenditure.

© 2010 Elsevier B.V. All rights reserved.

1. Introduction

Most of the current wireless sensor network (WSN) applications do not have high bandwidth demands, and are usually delay-insensitive. More recently, the technological advances in CMOS cameras and microphones have fostered the development of wireless multimedia sensor networks (WMSN) for many emerging applications such as multimedia surveillance sensor networks, advanced health care delivery, traffic avoidance, and person locator

services [1]. They will also increase the capabilities of traditional monitoring and surveillance systems by virtue of the distributed system of multiple cameras and sensors. Among these, wireless audio sensor networks (WASN), i.e., networks of wirelessly interconnected audio sensors, are also promising for the realization of efficient audio surveillance applications [2,3].

Communication of wide-band event signal such as audio signal containing high frequency components requires high transmission bandwidth. Once the event signal is sensed by a number of sensor nodes within the event radius, significant amount of traffic is injected to the network, which may easily cause severe packet losses and quick depletion of scarce network resource. Therefore,

* Corresponding author.

E-mail address: akan@ku.edu.tr (O.B. Akan).

in order to realize promising WASN applications, the additional communication challenges posed by the unique features of wide-band event signal, i.e., audio signal,¹ must be addressed. In the existing literature, there are many research efforts on reliable communication protocols that are devised for WSN domain and aim to efficiently communicate the event information to the sink [4–6]. Moreover, recently, a cross-layer rate control scheme is also introduced in order to fairly maximize the quality of the communicated multimedia streams by minimizing distortion [7]. However, the primary objective of these existing protocols is to achieve reliability and energy efficiency. They do not take the spectral characteristics of the event signal to be communicated into consideration in the determination of communication parameters. In fact, different event signal characteristics may need different treatment in terms of communication requirements such as different communication bandwidth demand and diverse reliability objectives. Furthermore, they do not address the communication of high-bandwidth event signals as in the case of WASN and do not perform or consider an exact reconstruction of the event signal from the delivered samples rather than averaged samples at the sink node.

On the other hand, due to the lack of the autonomous operations in these protocols, reliable sensor communication partially or fully depend on feedback messages from the sink. However, the feedback may not reach in time to provide reliable communication of event information and it may lead to waste of scarce network resources. Hence, it is imperative to develop an autonomous communication protocol for WASN that enables the sensor nodes to cooperatively and effectively communicate the event signal without the need for any coordination with the sink. This necessitates the sensor nodes to have the capability of self-organization rather than the control of a central entity such as the sink node or base station. With this self-organizing feature, the sensor nodes are expected to reliably communicate their readings with minimum energy expenditure despite any communication problems such as packet losses, link errors, and excessive delays so that *the sensor network operates in a relatively stable state*.

Similar to WASN, a major functionality of many biological organisms is the ability to autonomously maintain a relatively stable equilibrium state for the operation of vital functions [8]. This functionality is called *homeostasis*, and it is the principal quality of an organism to conserve its autonomy. Hence, this analogy between biological homeostasis and WASN gives inspiration to develop autonomous communication algorithm for WASN. The homeostasis-inspired autonomous communication (HAC) protocol devised for WASN is the main contribution of this work. The salient features of HAC are:

- HAC aims to communicate a sufficient number of data samples from the event signal to enable the exact reconstruction of the wide-band event signal with minimum energy expenditure.

- HAC aims to provide real-time communication of the wide-band event signal.
- HAC regulates its communication parameters according to the spectral characteristics of the event signal.
- HAC does not need any feedback message from the sink node.
- HAC allows the self-organization capability of the WASN, inspired by biological homeostasis, to maintain the sensor network in a relatively stable operating state in which the sensor nodes autonomously, reliably and, yet energy-efficiently communicate wide-band event signals to the sink.

The remainder of the paper is organized as follows. In Section 2, the network model and assumptions used in HAC protocol operation are introduced. In Section 3, biological homeostasis is reviewed and then, a connection between biological homeostasis and WASN is introduced. HAC algorithm is introduced in Section 4 based on the analogies between WASN and homeostasis given in Section 3. In Section 5, performance evaluation results of HAC are presented. Finally, concluding remarks are given in Section 6.

2. Network model and assumptions

We consider a network architecture in which the number of N audio sensors are deployed in an environment and they separately detect and communicate the event information to the sink node. Sensor nodes are assumed to use a fixed transmission power level. Therefore, they have a fixed transmission range, i.e., r , in which they communicate with each other. When an event occurs in the environment, the average number of S audio sensors that sense the audio signal act as source nodes to sample the event signal and generate data packets. This initiates the data transmission from sensor nodes to the sink node. The source nodes are assumed to form the average number of H clusters each of which has a cluster head. Each cluster head aggregates the source node packets and directly transmits to the sink node in one hop.

We assume that each sensor node uses a number of different frequency channels and selects and switches its radio front-end to one of these frequency channels in order to transmit and receive data packets. The selection of frequency channels used for the intra-cluster communication of sensor nodes is assumed to be made by cluster head. As will be introduced, HAC protocol allows the neighbor clusters, that may interfere with each other, to use different frequency channels. This aims to avoid high level of interference among the neighbor clusters. For the communication between cluster heads and the sink node, a single unique frequency channel, that is not used in intra-cluster communication of sensor nodes, is assumed to be set initially and used by the cluster heads to transmit the aggregated data packet to the sink node. Thus, the sink node also use the same frequency channel with the cluster heads in order to receive data packets from the cluster heads.

The wireless channel is assumed to be shared in fixed-duration time slots, which are, in turn, captured by sensor nodes in order to transmit. The duration of a time slot

¹ In this paper, we interchangeably use audio signal and event signal.

consists of two different intervals named packet transmission and acknowledgment (ACK) transmission interval. In the packet transmission interval, each sensor node transmits a packet to its destination and an ACK frame is transmitted back by the destination if the packet is successfully received. If at least two or more sensor nodes, that are in the communication range of each other, transmit using the same time slot, their packets collide and the current transmission attempt become unsuccessful.

3. Biological homeostasis and wireless audio sensor networks

In this section, the basic principles of biological homeostasis are first reviewed. Then, the analogies between biological homeostasis and WASN is presented, based on which HAC protocol is introduced.

3.1. Biological Homeostatic system

A vital functionality of many biological organisms is the ability to maintain a stable internal state although the environmental conditions may change rapidly [8]. This functionality is called *homeostasis*, and it is the leading feature of an organism to sustain its autonomy. By means of homeostasis, the organism self-regulates its growth and development, and maintains itself in the stable state. To sustain homeostatic stability within an organism, the nervous system, endocrine system, and immune system behave as one large, unified and complex system. The *interaction* and *communication* among all three systems are provided by the specific *receptors* on the cells [8].

A biological organism is open to various external stimuli. Neurons in the nervous system takes the stimuli, e.g., taste, smell, vision, etc., via the sensory parts, and triggers an output reaction at the effectors, e.g., tissues and muscles. After the nervous system detects an input stimulus, the endocrine system produces and releases hormones through *gland cells*. Thus, the interaction between the nervous and endocrine system is the homeostatic response behavior of the organism to sustain its stable internal state. Any *malfunction* that adversely affects the operation of the organism is detected by the *immune system* of the organism. The immune system is the defense mechanism for the maintenance of homeostatic stability. This system responds to foreign substances that are generally called *pathogens*. The response is applied through *B-cells* and *T-cells* of the adaptive immune system. B-cells and T-cells are white blood cells and have the capability to bind to and eliminate pathogenic material, i.e., *antigens*. In conclusion, there is a constant interaction among the neural, endocrine, and immune systems, and the collaboration of them provides a promising model for the construction and development of self-organizing, highly-functional, and adaptable intelligent systems.

3.2. Homeostasis-inspired wireless audio sensor networks

Similar to a biological homeostatic system, WASN must keep itself within a stable state for successful operation.

The stable state of a WASN corresponds to a network operating condition in which the sensor network autonomously, reliably, and yet energy-efficiently communicate a wide-band event signal at the sink despite any communication problems such as packet losses, link errors, and excessive delays. In WASN, the spectral characteristics of event signal impose a sampling frequency rate constraint on source nodes to enable successful reconstruction of the audio signal according to Nyquist Sampling Theory [10]. Spectral characteristics determine the total number of samples to be transmitted per unit time over the network and hence, the traffic load over the forward paths. When the traffic load over the network is excessively high, this leads to possible collisions and packet losses on the forward paths. Thus, it is required to estimate the spectral bandwidth of the event signal for energy efficient and reliable communication of sensor measurements. Similarly, in biological homeostasis, the properties of an external stimuli detected by neuron cells determine the response of organism to this external stimuli. When an external stimuli is detected by neuron cells, according to the properties of the external stimuli such as kind and the magnitude, neuron cells trigger the endocrine system to initiate the hormone secretion. Based on this similarity, we consider source nodes that sense and sample the event signal as neurons in neural system and call them as *N-Sensor*. Like a neuron in neural system, in WASN, the aim of an N-Sensor is to sense and sample the event signal and estimate the spectrum of the sensed event signal.

In endocrine system, gland cells are stimulated by neurons to secrete hormones so as to keep the organism in the biologically stable state. Similarly, in WASN, source nodes, i.e., N-sensors, form cluster to transmit event information to the cluster head in order to stimulate the cluster head for data transmission. Hence, we consider the cluster heads of the N-sensor clusters as gland cells and call them *G-Sensors*. In immune system, T-cells sense any malfunction in the organism and trigger the neural and endocrine systems to take an appropriate action. Similarly, in WASN, some sensor nodes must detect and notify any malfunction such as collisions and channel error and their symptoms such as

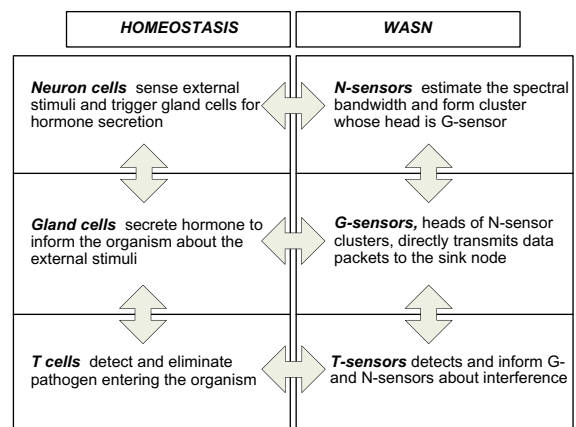


Fig. 1. The mapping between the homeostatic system elements and sensor networks.

packet losses and excessive delay. With this regard, we consider these sensor nodes that detect any malfunction in WASN as T-cells and call them as *T-sensors*. The analogies and the mappings between the homeostatic system elements and sensor networks are also outlined in Fig. 1. Note that each sensor node may jointly act as N-sensor, G-sensor, or T-sensor according to its current state such as source node and cluster head. Based on the analogies established in this section, in the next section, we present homeostasis-inspired Autonomous Communication (HAC) algorithm.

4. Homeostasis-inspired autonomous communication in WASN

HAC algorithm has several unique features which allow sensor nodes to collaboratively and effectively communicate the event information based on the principles of biological homeostasis as described in Section 3. HAC takes the spectral characteristics of the event signal into consideration in determination of the sampling and communication parameters used by sensor nodes. Based on the spectral bandwidth of the event signal estimated by the N-Sensor, HAC enables G-sensors to determine the number of samples which must be delivered in order to enable accurate reconstruction at the sink. Furthermore, it also provides significant energy conservation by means of an efficient sampling scheme named irregular sampling [9]. In this scheme, each N-sensor takes samples from the event signal with a probability (α) called *sampling probability* while it samples the event signal with sampling frequency f . A portion of irregularly sampled event signal is illustrated in Fig. 2. Since the irregular sampling scheme decreases the number of samples transmitted over the network by a sensor node, it decreases excessive traffic load which may cause possible packet losses, and therefore, it provides more accurate reconstruction at the sink with significant energy conservation [9]. The overall HAC operation is composed of five distinct phases as briefly introduced below:

1. *Spectrum estimation phase*: N-Sensor estimates the spectrum bandwidth of the event signal, i.e., B , to determine how many samples must be taken and delivered to satisfactorily reconstruct the event signal at the sink. HAC algorithm uses a periodogram-based Welch Method [11] to estimate the spectral bandwidth of the event signal. The details of this procedure is given in Section 4.1.

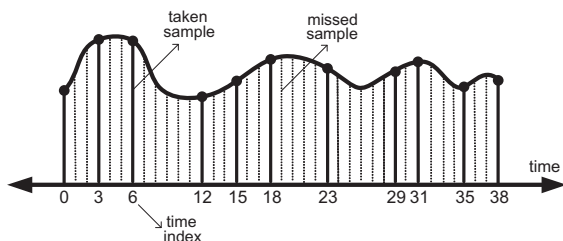


Fig. 2. A portion of irregularly sampled event signal.

2. *N-sensor clustering phase*: N-sensors form clusters according to their locational proximities with each other. Heads of the formed N-sensor clusters are selected as G-sensors to collect and directly transmit the data packets, received from N-sensors, to the sink as will be detailed in Section 4.2.
3. *Sampling probability determination phase*: G-sensors, i.e., cluster heads of N-sensor clusters, determine the sampling and communication parameters of N-sensors to ensure that a sufficient number of samples can be timely delivered to the sink node. This phase is elaborated in Section 4.3.
4. *Channel frequency selection phase*: In order to avoid excessive interference among neighbor N-sensor clusters, neighbor clusters select different operating frequency channels used for intra-cluster communication of sensor nodes. T-sensors detects frequency overlapping among neighbor clusters that use the same frequency channel and inform the clusters about that. Using this information, each cluster selects a different frequency channel in order to prevent excessive interference. This mechanism is explained in Section 4.4.
5. *Signal reconstruction phase*: The sink finally incorporates all samples of event signal, that are taken and delivered to the sink node, into a single sample set that is expected to include a sufficient number of samples that are needed for accurate reconstruction of the event signal. Detailed operation in this phase is introduced in Section 4.5. This phase completes the overall operation of HAC algorithm.

4.1. Spectrum estimation phase

N-sensors that sense and sample the event signal estimate the spectral bandwidth of the event signal $f_s(t)$ and obtain the bandwidth B . For the estimation of the event signal bandwidth, the N-sensor uses the periodogram-based Welch Method [11]. The details of the method is given in Appendix A.

4.2. N-sensor clustering phase

HAC allows N-sensors that are located in close proximities of each other to form clusters by selecting a cluster head. HAC also ensures that members of clusters sense correlated event signal due to the locational proximities. Here, we characterize the correlation among N-sensors by means of the correlation radius, i.e., c . If the distance between two N-sensors is less than c , these N-sensors are assumed to sense correlated event signal [12]. Moreover, without loss of generality, we also assume that the correlation radius of sensor nodes is less than their communication radius, i.e., $c < r$. This assumption ensures that each sensor node to be able to communicate with its correlated and non-correlated neighbors within its communication radius as shown in Fig. 3.

Each N-sensor i decides whether or not to become a cluster head by sending *Request To Cluster* (RTC) message with a probability p at the beginning of each time slot. When N-sensor i sends a RTC message, N-sensors that are in the correlation radius of N-sensor i and receive the

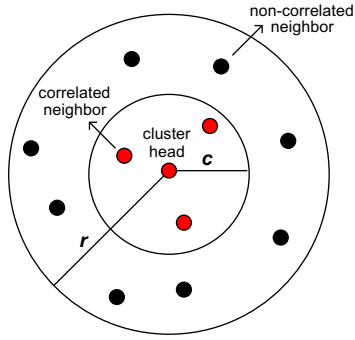


Fig. 3. Illustration of correlated and non-correlated neighbors around a cluster head.

RTC message form a cluster whose head is N-sensor i . In order to provide quick formation of the clusters that is required for the real-time communication, it is essential to avoid possible collision of RTC messages. The optimal selection of p can provide an optimal performance in the cluster formation phase. HAC provides a nearly-optimal solution for the cluster formation phase as follows. We assume that the cluster formation is initiated with the detection of an event signal by N-sensors. We also assume that the event signal is detected in time slot 1 and N-sensor i has $n(k)$ neighbors that are neither a cluster head nor a member of a cluster at the k th slot. In this case, the expected number of time slots during which N-sensor i successfully transmits a RTC message and becomes a cluster head, i.e., C , can be given as

$$C = \sum_{k=1}^{\infty} kp(1-p)^{n(k)}[1-p(1-p)^{n(k)}]^{k-1} \quad (1)$$

The computation of C clearly depends on the statistical properties of $n(k)$ such as mean and variance. However, if a mean estimate for $n(k)$, i.e., \hat{n} , is available, an approximation for C , i.e., \hat{C} , can be given as

$$\hat{C} = \sum_{k=1}^{\infty} kp(1-p)^{\hat{n}}[1-p(1-p)^{\hat{n}}]^{k-1} \quad (2)$$

In this case, \hat{C} can be computed as

$$\hat{C} = \frac{1}{R} \quad (3)$$

where $R = p(1-p)^{\hat{n}}$ and \hat{C} is a strictly decreasing function of R . Thus, \hat{C} can be minimized by maximizing R . Since R is a concave function of p , it has a global maximum for the optimal p , i.e., p_{opt} , obtained by solving

$$\frac{\partial R}{\partial p} = (1-p)^{\hat{n}} - p\hat{n}(1-p)^{\hat{n}-1} = 0 \quad (4)$$

Hence, the optimal RTC transmission probability, i.e., p_{opt} , that minimizes the average formation time of a cluster, i.e., \hat{C} , can be given as

$$p_{opt} = \frac{1}{\hat{n}} \quad (5)$$

Surely, \hat{n} has to be determined in order to find p_{opt} . However, \hat{n} depends on some system parameters such as

desired number of cluster heads and the average number of time slots during which overall clustering process is expected to be completed. If we assume that the overall clustering phase is completed within K slots, using the Markov inequality, an upper bound for the probability, that an N-sensor cannot become a cluster head, can be given as

$$\Pr(C \geq K) \leq \frac{E[C]}{K} \quad (6)$$

By substituting $E[C] = \hat{C}$ in (6), it can be rewritten as

$$\Pr(C \geq K) \leq \frac{\hat{C}}{K} \quad (7)$$

Using the upper bound in (7), it is expected that at least

$$H = S \left(1 - \frac{\hat{C}}{K}\right) \quad (8)$$

number of N-sensors becomes cluster head at the end of an N-sensor clustering phase. If we assume that S , H , and K are known a priori by the system setting, \hat{C} can be computed as

$$\hat{C} = K \left(1 - \frac{H}{S}\right) \quad (9)$$

By substituting \hat{C} , computed in (3), (9) can be rewritten as

$$p(1-p)^{\hat{n}} = \frac{S}{K(S-H)} \quad (10)$$

As presented above, the optimal p , i.e., $p_{opt} = \frac{1}{\hat{n}}$, minimizes the expected number of slots in which an N-sensor becomes a cluster head, i.e., \hat{C} . Thus, by setting $p = p_{opt}$, (10) can be written as

$$\frac{1}{\hat{n}} \left(1 - \frac{1}{\hat{n}}\right)^{\hat{n}} = \frac{S}{K(S-H)} \quad (11)$$

HAC enables each N-sensor to determine \hat{n} by iteratively solving (11) that has two real roots for $0 < \frac{S}{K(S-H)} < 1$. One root of (11) is near 1 and the other is greater than 1. The root, that is nearly 1, i.e., $\hat{n} \approx 1$, is not proper for our case because this makes $p_{opt} \approx 1$. However, the other root, that is greater than 1, i.e., $\hat{n} > 1$, is a proper one. In Fig. 4a, for different $\frac{S}{K(S-H)}$ values, the numerically computed \hat{n} values are shown. HAC provides a simple iterative procedure followed by all N-sensors to determine an approximate \hat{n} by iteratively testing (11) as follows:

- By substituting $\hat{n} = 1, 2, \dots, b$, find the numerical value for the left side of (11) and collect them as F_1, F_2, \dots, F_b , respectively, where b is a sufficiently high upper bound for \hat{n} that is set a priori.
- Compute the errors as $E_i = |F_i - \frac{S}{K(S-H)}|$ for $i = 1, 2, \dots, b$.
- Find the minimum E_i , $i \in \{1, 2, \dots, b\}$ and set its index as $\hat{n} = i$, where E_i is the minimum.

In Fig. 4b, the above iterative procedure is illustrated to find \hat{n} for $\frac{S}{K(S-H)} = 0.03$. As observed in the data cursor, \hat{n} is found as 11, which gives a satisfactory approximation to $\frac{S}{K(S-H)} = 0.03$. The numerical solution of (11) is very close to the iteratively obtained solution. The numerical solution is equal to $\hat{n} = 11.720$ while the iterative solution is

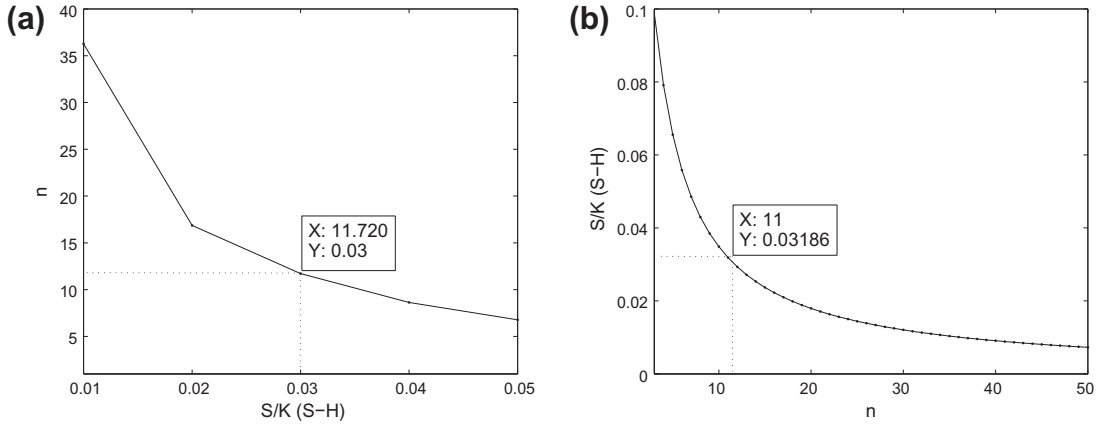


Fig. 4. (a) \hat{n} is shown for different $\frac{S}{K(S-H)}$ values. (b) By substituting $\hat{n} = 1, 2, \dots, b$, numerical values for the left side of (11) is shown.

$\hat{n} = 11$. Consequently, HAC allows N-sensors to form a desired number of clusters within a desired cluster formation time. Moreover, despite the fact that cluster heads are severely energy consuming node, HAC also provides a uniformly distributed energy consumption for N-sensors by selecting cluster heads among all N-sensors with the same probability, i.e., p_{opt} .

4.3. Sampling probability determination phase

As introduced in Section 4, HAC uses the irregular sampling scheme in which each N-sensor takes a sample from event signal with probability α while it samples the event signal with the sampling frequency f . Each cluster head of N-sensor clusters acts as a G-sensor to determine α in its cluster. Using α , the probability that a specific sample of the event signal, i.e., $Sample_k$, is taken ($P[Sample_k \text{ is taken}]$) at least by one N-sensor is expressed by

$$P[Sample_k \text{ is taken}] = [1 - (1 - \alpha)^M] \quad (12)$$

where M is the number of members in the cluster. If the sampling frequency determined by the cluster head, i.e., G-sensor, is f (Hertz), then the total number of samples taken (in a second) is $f \cdot P[Sample_k \text{ is taken}]$. On the other hand, the expected number of the N-sensors which take any sample, i.e., D , can be given as

$$D = \sum_{i=0}^M i \binom{M}{i} \alpha^i (1 - \alpha)^{M-i} \quad (13)$$

D is also the mean of the binomial distribution $B(M, \alpha)$, and can be expressed as $D = \alpha M$. Consequently, the average number of distinct samples delivered to the G-sensor, i.e., N_d , can be given as

$$N_d = (1 - \lambda) f [1 - (1 - \alpha)^M] \quad (14)$$

where λ is the packet loss probability observed by the cluster head, i.e., G-sensor. According to the Nyquist sampling theorem, if the event signal has bandwidth B^2 in Hertz, it is

imperative for N-sensors to take more than B number of distinct samples (N_d) within a second to satisfactorily reconstruct the event signal at the sink node, that is,

$$N_d > B \quad (15)$$

must be satisfied for the reconstruction. N_d is a function of α , f , M , and λ . Among these, λ is affected by many factors such as channel access scheme of N-sensors and signal-to-noise ratio in the sensor channels. HAC algorithm enables each G-sensor to optimize its channel access and the channel accesses of N-sensors in its cluster. For this optimization, G-sensors determine two channel access probabilities, i.e., p_a and p_c , to provide real-time delivery for samples of event signal. p_a is the channel access probability that each N-sensor in the cluster transmits to the cluster head at the beginning of each time slot. Similarly, p_c is the channel access probability that each cluster head transmits to the sink node at the beginning of each time slot. Here, we assume that the packet losses may arise from possible collisions and channel errors. After a packet is exposed to a specific number of unsuccessful transmission attempts due to possible collisions and channel errors, it is assumed to be dropped. Possible collisions are affected by the channel access probabilities p_a and p_c while channel errors can be characterized by a packet failure probability p_f given as [13]

$$p_f = 1 - \left(1 - 0.5e^{-\frac{\gamma}{1.28}}\right)^{8\kappa} \quad (16)$$

where γ is signal-to-noise ratio and κ is the number of samples³ in a packet. The packet losses in the network may be experienced in the links either between N-sensors and G-sensor or between G-sensors and the sink node. Thus, the packet loss probability λ given in (14) consists of the summation of two independent packet loss probabilities, i.e., λ_a and λ_c , that is, $\lambda = \lambda_a + \lambda_c$. λ_a is the packet loss probability observed in the link between N-sensors and the cluster

² Here, the spectral bandwidth of the event signal is defined as the twice of its maximum frequency component.

³ In this paper, without loss of generality, we assume that each sample of the event signal is quantized by eight bits.

head, i.e., G-sensor. Using p_a and p_f , the packet loss probability λ_a can be expressed as

$$\lambda_a = [1 - p_a(1 - p_f)(1 - p_a)^{M-1} - (1 - p_a)^M]^{z+1} \quad (17)$$

where z is allowable unsuccessful transmission attempts for a packet before it is dropped. Similarly, λ_c is the packet loss probability observed in the link between G-sensors and the sink node and using p_c and p_f , it can be expressed as

$$\lambda_c = [1 - p_c(1 - p_f)(1 - p_c)^{H-1} - (1 - p_c)^H]^{z+1} \quad (18)$$

where H is the average number of cluster heads in the network as introduced in Section 4.2. Consequently, the overall packet loss probability λ can be expressed as $\lambda = \lambda_a + \lambda_c$. In addition to the packet loss probability, using p_a and p_c , expected number of time slots required for a successful delivery of a packet from an N-sensor to the cluster head and from the cluster head to the sink node, i.e., ξ_a and ξ_c , respectively, can be also given as

$$\begin{aligned} \xi_a &= \sum_{i=0}^{\infty} i S_a (1 - S_a)^{i-1} = \frac{1}{p_a(1 - p_a)^{M-1}} \quad \text{and} \\ \xi_c &= \sum_{i=0}^{\infty} i S_c (1 - S_c)^{i-1} = \frac{1}{p_c(1 - p_c)^{H-1}} \end{aligned} \quad (19)$$

where S_a is the successful delivery probability of a packet transmitted from an N-sensor to the cluster head and given as $S_a = p_a(1 - p_a)^{M-1}$. Similarly, S_c is the successful delivery probability of a packet transmitted from a cluster head to the sink node and given as $S_c = p_c(1 - p_c)^{H-1}$. Hence, the expected number of time slots required for a successful delivery of a packet, i.e., ξ , can be given as the summation of ξ_a and ξ_c , i.e., $\xi = \xi_a + \xi_c$.

Here, we assume that ξ has to be less than or equal to the expected packet generation time of an N-sensor in order to provide real-time communication of event information. Each N-sensor takes sample with sampling probability α while it samples the event signal with sampling frequency f . Thus, each N-sensor takes $\alpha f \tau$ samples during a slot time, i.e., τ . Since a data packet is assumed to include κ samples from the event signal, the expected number of time slots during which a packet is generated by an N-sensor, i.e., η , can be given as

$$\eta = \frac{\kappa}{\alpha f \tau} \quad (20)$$

Hence, for the real-time communication of event information, it must be satisfied that

$$\xi = \xi_a + \xi_c \leq \eta \quad (21)$$

$$\frac{1}{p_a(1 - p_a)^{M-1}} + \frac{1}{p_c(1 - p_c)^{H-1}} \leq \frac{\kappa}{\alpha f \tau} \quad (22)$$

As observed in (22), the channel access probabilities p_a and p_c are implicitly a function of κ , τ , H , M , α , and f . Among these, κ , τ , H , and M , are assumed to be known while α and f are optimized by HAC protocol operation to satisfy the conditions given in (15) and (22). While doing this, HAC also tries to provide the minimum energy consumption. Energy consumption is mostly affected by the data traffic generated by N-sensors over the network. More

specifically, since each N-sensor takes the average number of αf samples in a second and each packet includes the same number of samples, αf determines the average reporting frequency rate of sensor nodes (packets/s.) and thus, energy consumption rate over the network. Hence, in order to minimize energy consumption rate in the network, HAC aims to minimize αf . In fact, incorporating the conditions given in (15) and (22) into this objective, sampling probability determination phase of HAC can be modeled by an optimization process given as

minimize αf

$$\begin{aligned} \text{subject to } N_d > B \quad \text{and} \quad & \frac{1}{p_a(1 - p_a)^{M-1}} \\ & + \frac{1}{p_c(1 - p_c)^{H-1}} \leq \frac{\kappa}{\alpha f \tau} \end{aligned} \quad (23)$$

Using some specific relation among the parameters such as α , λ , and N_d , HAC allows G-sensors to iteratively solve the optimization problem modeled in (23) as follows. The successful packet delivery probabilities $S_a = p_a(1 - p_a)^{M-1}$ and $S_c = p_c(1 - p_c)^{H-1}$ are the concave function of p_a and p_c , respectively. Therefore, S_a and S_c have a global maximum at $p_a = \frac{1}{M}$ and $p_c = \frac{1}{H}$. Using the global maximum values of them, the condition required for the real-time communication and given in (22) can be rewritten as

$$\frac{1}{\frac{1}{M}(1 - \frac{1}{M})^{M-1}} + \frac{1}{\frac{1}{H}(1 - \frac{1}{H})^{H-1}} \leq \frac{\kappa}{\alpha f \tau} \quad (24)$$

By rearranging, (24) can be written as

$$\frac{\frac{\kappa}{\tau M H} (1 - \frac{1}{M})^{M-1} (1 - \frac{1}{H})^{H-1}}{\left[(1 - \frac{1}{M})^{M-1} + (1 - \frac{1}{H})^{H-1} \right]} \geq \alpha f \quad (25)$$

Clearly, (25) provides an upper bound for αf that is tried to be minimized by HAC protocol operation. f also has a lower bound at B since the event signal has the spectral bandwidth B according to Nyquist sampling theory. On the other hand, since p_a and p_c are selected from the interval $0 < p_a \leq \frac{1}{M}$ and $0 < p_c \leq \frac{1}{H}$, respectively, the packet loss probabilities, i.e., λ_a and λ_c are the strictly increasing function of p_a and p_c , respectively. Hence, substituting $p_a = \frac{1}{M}$ and $p_c = \frac{1}{H}$ into (17) and (18), respectively, the worst case packet loss probabilities, i.e., $\bar{\lambda}_a$ and $\bar{\lambda}_c$, can be expressed as

$$\bar{\lambda}_a = \left[1 - \frac{(1 - p_f)}{M} \left(1 - \frac{1}{M} \right)^{M-1} - \left(1 - \frac{1}{M} \right)^M \right]^{z+1} \quad (26)$$

$$\bar{\lambda}_c = \left[1 - \frac{(1 - p_f)}{H} \left(1 - \frac{1}{H} \right)^{H-1} - \left(1 - \frac{1}{H} \right)^H \right]^{z+1} \quad (27)$$

Combining $\bar{\lambda}_a$ and $\bar{\lambda}_c$, the overall worst case packet loss probability can be found as $\bar{\lambda} = \bar{\lambda}_a + \bar{\lambda}_c$. N_d is a strictly decreasing function of λ . Thus, using the worst case packet loss probability $\bar{\lambda}$, a worst case realization of N_d , i.e., \bar{N}_d , can be expressed as

$$\bar{N}_d = (1 - \bar{\lambda}^{M\alpha}) f (1 - (1 - \alpha)^M) \quad (28)$$

\bar{N}_d is also a strictly increasing function of α for $0 < \alpha \leq 1$. In order to show this, the first derivative of \bar{N}_d with respect to α , i.e., $\frac{\partial \bar{N}_d}{\partial \alpha}$, can be given as

$$\frac{\partial \bar{N}_d}{\partial \alpha} = M(1 - \alpha)^{M-1} (1 - \bar{\lambda}^{\alpha M}) - M \log(\bar{\lambda}) (1 - (1 - \alpha)^M \bar{\lambda}^{\alpha M}) \quad (29)$$

As observed in (29), $\frac{\partial \bar{N}_d}{\partial \alpha}$ is clearly positive for $0 < \alpha \leq 1$, which renders \bar{N}_d strictly increasing function of α . Hence, $N_d > B$ is always satisfied if an appropriate α and f , that satisfy (25) and provides $\bar{N}_d > B$, can be found. Consequently, since \bar{N}_d is a strictly increasing function of α , by using the upper bounds for α and f given in (25), a nearly-optimal solution for the optimization problem given in (23) can be provided by HAC protocol operation as follows.

Each G-sensor initially computes the worst case packet loss probability $\bar{\lambda} = \bar{\lambda}_a + \bar{\lambda}_c$ using (26) and (27). Then, it selects the minimum sampling frequency f that satisfies (25) and $f > B$. Using the selected f , it iteratively searches for the minimum sampling probability α that provides $\bar{N}_d > B$ as follows. Since \bar{N}_d is a strictly increasing function of α , this search can be performed by iteratively increasing α and testing whether or not $\bar{N}_d > B$ is satisfied. Here, we assume that starting with a sufficiently small value, α is increased by as $\alpha + \delta$ in each iteration, where δ is a sufficiently small step size.⁴ In the iterative search, if the current α provides $\bar{N}_d > B$, it is immediately selected as the sampling probability of N-sensors. If there is no such an α value satisfying the conditions, f is updated using a sufficiently small positive step size⁵ ζ as $f + \zeta$ and the same procedure is followed using the updated f until the minimum α that is in $0 < \alpha \leq 1$ and provides $\bar{N}_d > B$ is found. The sampling probability determination phase of HAC is also presented in Algorithm 1. After the determination of α and f , HAC also computes the minimum channel access probability p_a that satisfy the condition given in (22). The channel access probability of all cluster heads, i.e., p_c , is assumed to be set as $p_c = \frac{1}{H}$ by HAC protocol operation.

Algorithm 1. HAC: Sampling probability determination phase

```

1  for each Each G-Sensor do
2    computes  $\bar{\lambda} = \bar{\lambda}_a + \bar{\lambda}_c$ 
3    selects the minimum  $f$  satisfying (25) and
    $f > B$ 
4    while  $\bar{N}_d < B$  do
5      updates  $\alpha$  as  $\alpha + \delta$ 
6    end
7    if an  $\alpha$  that provides  $\bar{N}_d > B$  can be found then
8      selects this  $\alpha$  as the sampling probability
9    else
10     updates  $f$  as  $f + \zeta$  and go to line 4
11   end
12 end
13 end

```

⁴ The initial value of α and the step size δ are set as 0.001 in the numerical analysis of this paper.

⁵ ζ is set as $\zeta = 1$ in the numerical results.

4.4. Channel frequency selection phase

HAC enables each cluster of N-sensors to use different frequency channels in order not to interfere with each other. This can be achieved by means of feedback messages from T-sensors. T-sensors are the sensor node that are located at the overlapping areas of the N-sensor clusters. In Fig. 5, two clusters, i.e., cluster 1 and 2, are shown. They have an overlapping area in which there are four T-sensors. T-sensors in this region clearly receives N-sensor transmissions from both clusters if these clusters use the same frequency channel. Therefore, they recognize whether or not these two clusters use the same frequency channel. If they use the same channel, this imposes a high level of interference on the communication in these cluster. In order to avoid this high interference level, HAC enables T-sensors to change the operating frequency channel used in the neighbor clusters as follows.

Since T-sensors are also in the communication range of each other, they first determine two different frequency channel IDs and sends these IDs to the cluster heads. If the cluster heads accept these channels, they immediately switches to these new channels. Even if one of the cluster heads does not accept the new frequency channels, T-sensors find two new frequency channel IDs to send the cluster heads. The acceptance of the newly proposed frequency channels depends on whether or not cluster heads already have some neighbor clusters that use these channels. If such a situation is not arisen, the proposed frequency channels are immediately accepted by the cluster heads for the intra-cluster communication. Moreover, once a cluster head switches to a proposed frequency channel, it does not change this channel anymore. This mechanism prevents a cluster head to uncertainly oscillate different frequency channels.

4.5. Signal reconstruction phase

In this phase, the sink node forms the complete sample set of the event signal $f_s(t)$ using the samples generated and transmitted by N-sensors using sampling frequency f and sampling probability α . Here, we assume that each N-sensor i also generates and transmit an indicator set I_i

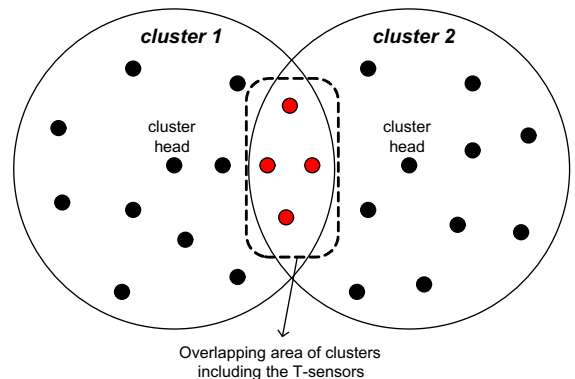


Fig. 5. Two clusters, i.e., clusters 1 and 2, with their overlapping area including a number of T-sensor.

Table 1
Evaluation parameters.

Number of sensors in the network (N)	100
Number of sensors in a cluster (M)	5–25
Number of clusters (H)	4–10
Event signal bandwidth (B)	4–10 kHz
Packet size (κ)	50 samples
Slot duration (τ)	0.0001 (s)
Packet failure probability (p_f)	0.01

for its packets to inform the sink node about which samples are taken from $f_s(t)$ by it. I_i is a vector that includes 1 for the taken samples and includes 0 for the missed samples. Hence, using I_i , the sink node knows which samples are taken by N-sensor i during a sampling interval T (s) if the data packet including these samples and their indicator set is received. If I_i is not received with a data packet, indicator set of this packet is set as 0. Furthermore, I_i is simply transmitted as a $\lceil fT \rceil$ length bit stream because it includes a string of 0 and 1 bits. Therefore, the usage of I_i incurs a considerably low transmission overhead. In the sink node, the sample set generated and transmitted by N-sensor i , i.e., K_i , can be given as

$$K_i = [I_i(1)f_s(0), I_i(2)f_s\left(\frac{1}{f}\right), \dots, I_i(\lceil fT \rceil)f_s(T)] \quad (30)$$

The sink node combines the sampling sets of all N-sensors, i.e., K_i , $\forall i$, to generate a complete sample set of event signal, i.e., \bar{K} . Then, the sink node reconstructs the event signal $f_s(t)$ using the complete sample set \bar{K} . Here, the reconstruction method of the signal is not in the scope of this paper. We only assume that the event signal can be reconstructed from the complete sample set of the event signal if a sufficient number of distinct samples can be taken and delivered to the sink by N-sensors.

5. Numerical results

In this section, we numerically analyze the performance of HAC algorithm. We assume that the total number of N sensor nodes are deployed in a WASN environment and by means of the N-sensor clustering phase, N-sensors form H number of clusters whenever an event signal is detected in the environment. Each cluster is assumed to include M N-sensors. Moreover, the bandwidth of the event signal may change from 4–10 kHz. The parameters used in the numerical results are given in Table 1. The analysis are

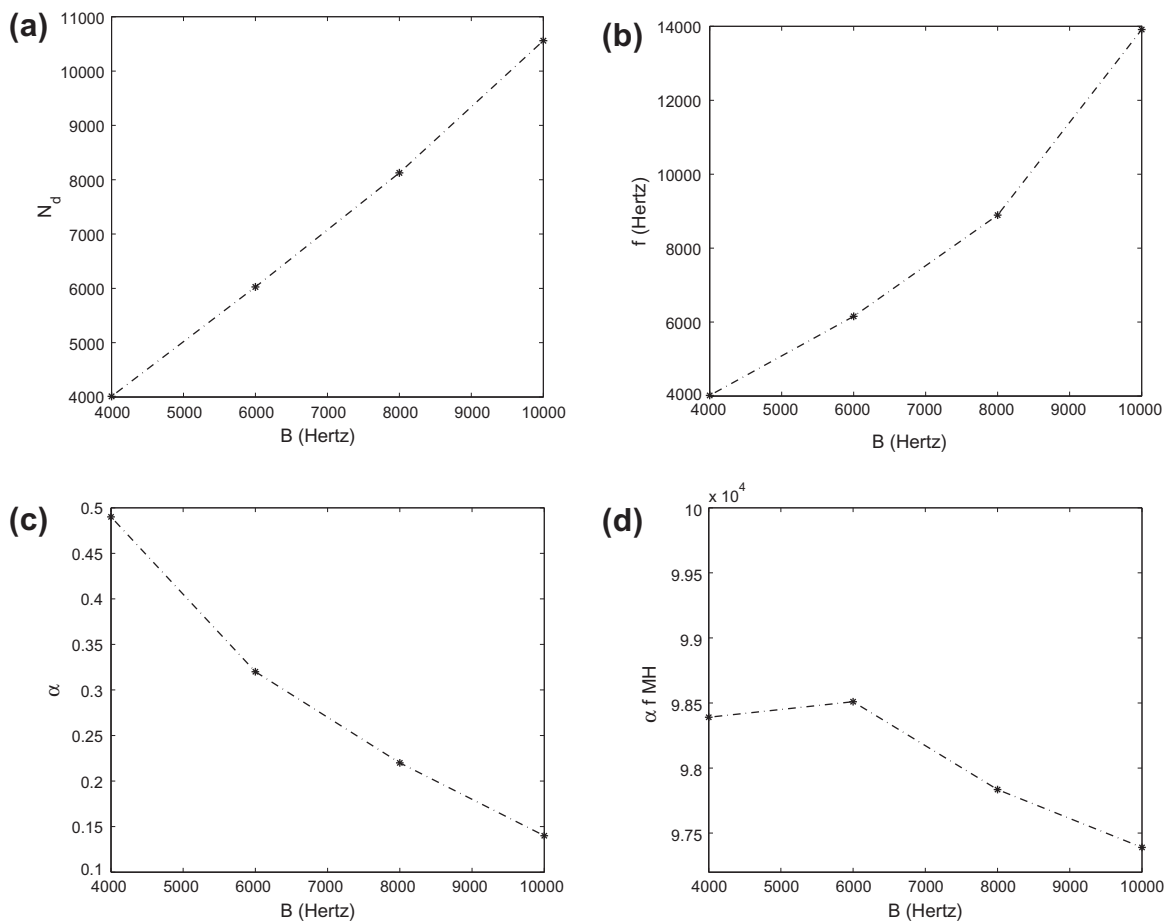


Fig. 6. (a) The average number of distinct samples delivered within a second, i.e., N_d , is shown with the event signal bandwidth, i.e., B , values. (b) f is shown with B . (c) α is shown with B . (d) The total number of samples taken by all N-sensors during a second, i.e., $\alpha f MH$, is shown with B .

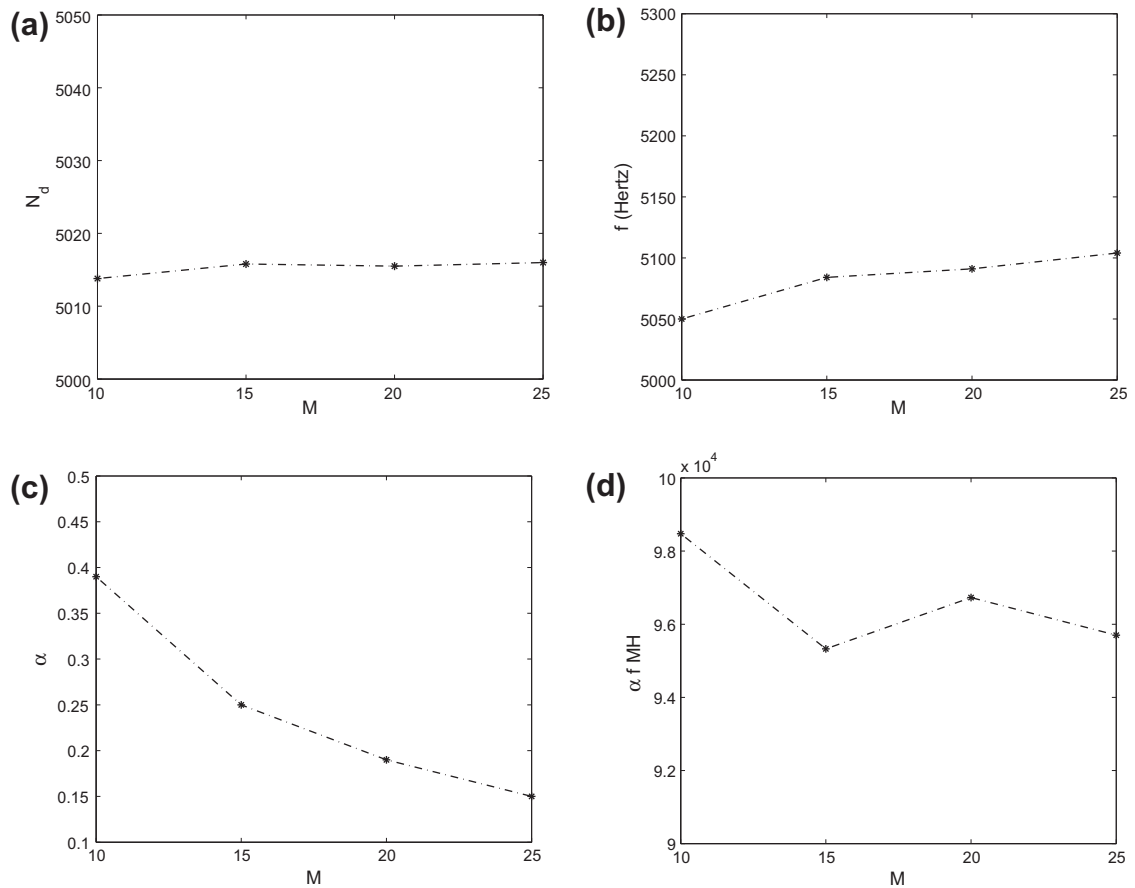


Fig. 7. (a) The average number of distinct samples delivered within a second, i.e., N_d , is shown with the number of members in a cluster, i.e., M . (b) f is shown with M . (c) α is shown with M . (d) The total number of samples taken by all N-sensors during a second, i.e., $\alpha f MH$, is shown with M .

evaluated by using MATLAB. The performance of the HAC algorithm is investigated by numerically evaluating the performance of *sampling probability determination phase*.

In Fig. 6, assuming that the number of $H = 5$ clusters each of which includes $M = 10$ N-sensors are formed in the N-sensor clustering phase, we change the event signal bandwidth from $B = 4$ kHz to $B = 10$ kHz in order to show the effect of B on the performance of HAC. In Fig. 6a, the number of distinct samples delivered to the sink node within a second, i.e., N_d , is shown. As B increases, N_d is increased by HAC protocol operation such that N_d is slightly more than the event signal bandwidth B . This enables the exact reconstruction of event signal at the sink node while providing the delivery of minimum number of samples and thus, the minimum energy consumption of sensor nodes. Similarly, as B increases, f is increased by HAC protocol operation. For each event signal bandwidth B , HAC provides a different f that is slightly more than B .

On the other hand, for the same case, as B increases, the sampling probability α is reduced by HAC protocol operation as shown in Fig. 6c. This is because sampling frequency increases with the event signal bandwidth B . As f increases with B , HAC allows N-sensors to increase the number of distinct samples taken from the event signal

by using lower sampling probabilities. This also causes a significant improvement in the energy conservation rate of the sensor nodes. In order to show the energy consumption rate of the sensor nodes, in Fig. 6d, the expected number of samples taken by all N-sensors in the network within a second, i.e., $\alpha f MH$ is shown. As observed, $\alpha f MH$ slightly changes although the bandwidth B changes from $B = 4$ kHz to $B = 10$ kHz. This can be achieved by decreasing the sampling probability α as seen in Fig. 6c. This results shows the significant energy conservation capability of HAC.

Similarly, in Fig. 7, the effects of the number of members in the clusters, i.e., M , on the performance of HAC are shown. In Fig. 7a, the number of distinct samples delivered in a second, i.e., N_d , is shown with M . As M increases, the contention on the channel of the cluster head increases. However, HAC enables the network to deliver a sufficient number of samples that is slightly higher than the event signal bandwidth ($B = 5$ kHz). The sampling frequencies (f) nearly over the bandwidth are also selected by HAC protocol operation as shown in Fig. 7b. However, in contrary to N_d and f , the sampling frequency α is decreased by HAC as M increases. This stems from the increase in the diversity of the N-sensor samples such that

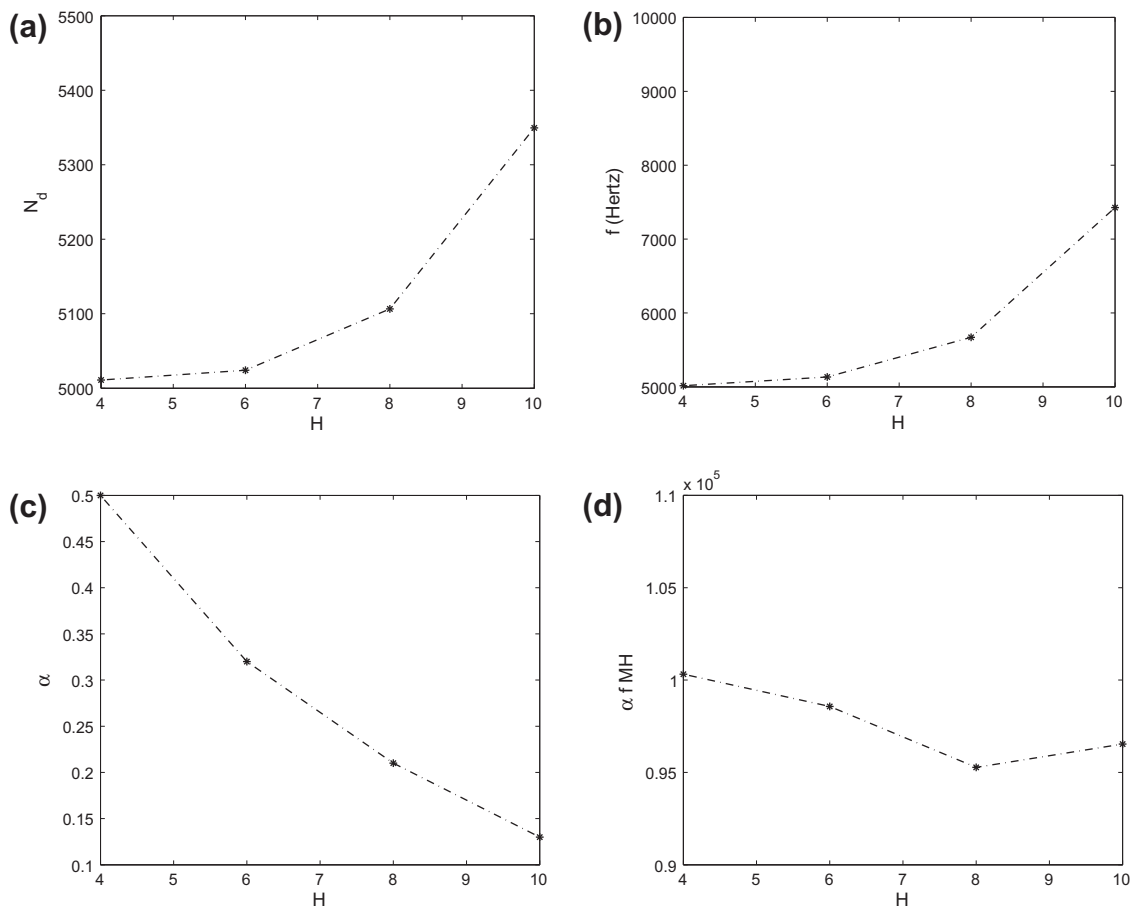


Fig. 8. (a) The average number of distinct samples delivered within a second, i.e., N_d , is shown with the number of clusters in the network, i.e., H . (b) f is shown with H . (c) α is shown with H . (d) The total number of samples taken by all N -sensors during a second, i.e., $\alpha f MH$, is shown with H .

as M increases, N -sensors can take sufficient number of samples, that is slightly more than B , using lower sampling probability. As observed in Fig. 7d, by reducing α , HAC also maintain the average number of samples taken over the network during a second, i.e., $\alpha f MH$, in a nearly constant level regardless of the increase in the M . This provides a significant energy conservation for sensor nodes such that

the energy consumption rate of the network remain almost the same regardless of the increase in M .

In Fig. 8, the effect of the average number of clusters in the network, i.e., H , on the performance of HAC is shown. N_d is shown with H in Fig. 8a. While H increases from 2 to 10, which increases the number of N -sensors in the network 10 times, N_d slightly increases over 5000 that is the event signal bandwidth in Hertz. Similarly, in Fig. 8d, the total number of samples taken by all N -sensors within a second also remain almost the same level, which gains significant energy conservation over the network. This provides a great stability that remains the data traffic in an almost the same level. This can be achieved by HAC protocol operation reducing the sampling probability α as shown in Fig. 8c.

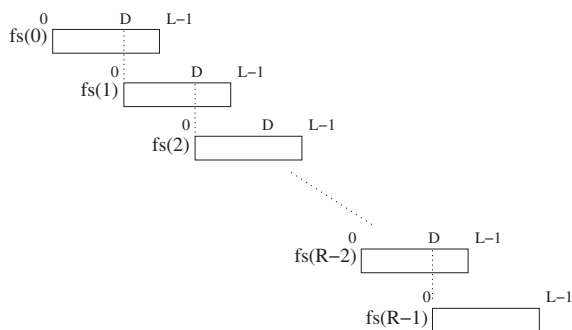


Fig. 9. Overlapping Samples.

6. Conclusion

In this paper, the homeostasis-inspired autonomous communication (HAC) protocol for wireless audio sensor networks (WASN) is introduced. Using the spectral properties of the event signal, the aim of HAC is to enable sensor nodes to achieve energy- and bandwidth-efficient

communication of the event signal, i.e., audio signal, without any need for feedback messages from the sink node. Using the irregular sampling mechanism, HAC significantly improves the energy conservation performance of the network while it also ensures that a sufficient number samples needed for exact reconstruction according to Nyquist sampling theory is timely delivered to the sink node. Due to these unique features of HAC, it can provide an efficient communication solution for event signals with high frequency components. Moreover, HAC provides highly reliable and autonomous event-to-sink data communication based on the interactions of the network components inspired by the elements of a biological homeostatic system.

Appendix A

Each N-Sensor estimates the spectral characteristics of the event signal $f_s(t)$ in the following way:

- It initially senses $f_s(t)$ and generates a sample set $f_s(0)f_s(1), \dots, f_s(R-1)$.
- It takes length L sample segments, having overlapping samples as shown in Fig. 9, from the sample set such that each segment has D units apart such that $D < L$. Let $f_s^1(j)$ be the first segment, then

$$f_s^1(j) = f_s(j), j = 0, 1, \dots, L-1$$

$$f_s^2(j) = f_s(j+D), j = 0, 1, \dots, L-1$$

⋮

$$f_s^K(j) = f_s(j+(K-1)D), j = 0, 1, \dots, L-1$$

where K denotes the number of segments. All samples in the segments cover the entire signal $((K-1)D+L=R)$.

- It selects a data window denoted as $W(j)$, $j = 0, 1, \dots, L-1$.
- Using the data window $W(j)$, it forms the sequence $f_s^1(j)W(j), \dots, f_s^K(j)W(j)$. Then, it takes Fourier transform $A_1(n), \dots, A_K(n)$ of these sequences such that

$$A_k(n) = \frac{1}{L} \sum_{j=0}^{L-1} f_s^k(j)W(j)e^{-2Kijn/L}$$

where $i = \sqrt{-1}$.

- It obtains K modified periodograms such that

$$I_k(f_n) = \frac{L}{U} |A_k(n)|^2, k = 1, 2, \dots, K$$

where $f_n = \frac{n}{L}$, $n = 0, \dots, \frac{L}{2}$ and $U = \frac{1}{L} \sum_{j=0}^{L-1} W(j)^2$.

- It computes the estimate of power spectral density of $f_s(t)$ as the average of these K periodograms ($I_k(f_n)$) as follows

$$\hat{P}(f_n) = \frac{1}{K} \sum_{j=1}^K I_j(f_n). \quad (31)$$

- It detects the maximum frequency component f_{max} of $f_s(t)$, which satisfies $f_{max} < \frac{L}{2}$. Thus, the spectral bandwidth of $f_s(t)$ is equal to $B = 2f_{max}$.

To update the spectral information of the event signal, each N-Sensor repeats above spectrum estimation procedure in each time interval τ .

References

- [1] I.F. Akyildiz, T. Melodia, K.R. Chowdhury, A survey on wireless multimedia sensor networks, *Computer Networks* 51 (4) (2007) 921–960.
- [2] E. Gurses, O.B. Akan, Multimedia communication in wireless sensor networks, *Annals of Telecommunications* 60 (7–8) (2005) 799–827.
- [3] S. Misra, M. Reisslein, G. Xue, A survey of multimedia streaming in wireless sensor networks, *IEEE Communications Surveys and Tutorials* 10 (4) (2008) 18–39.
- [4] O.B. Akan, I.F. Akyildiz, Event-to-sink reliable transport in wireless sensor networks, *IEEE/ACM Transactions on Networking* 13 (2005) 1003–1016.
- [5] C. Wan, S.B. Eisenman, A.T. Campbell, CODA: congestion detection and avoidance in sensor networks, in: *Proceedings of the ACM Sensys 2003*, Los Angeles, USA, November 2003.
- [6] F. Stann, J. Heidemann, RMST: reliable data transport in sensor networks, in: *Proceedings of the ACM MobiHoc 2004*, Roppongi, Japan, May 2004.
- [7] S. Pudlewski, T. Melodia, A distortion-minimizing rate controller for wireless multimedia sensor networks, *Computer Communications* 33 (12) (2010) 1380–1390.
- [8] M. Neal, J. Timmis, Once more unto the breach towards artificial homeostasis, in: *Recent Advances in Biologically Inspired Computing*, IGP, pp. 340–365.
- [9] B. Atakan, O.B. Akan, On Event Signal Reconstruction in Wireless Sensor Networks, in: *Proceedings of the IFIP/TC6 NETWORKING 2007*, Atlanta, GA, May 2007.
- [10] A.V. Oppenheim, R.W. Schaffer, J.R. Buck, *Discrete-Time Signal Processing*, Prentice Hall, 1999.
- [11] P.D. Welch, The use of fast Fourier transform for the estimation of power spectra: a method based on time averaging over short modified periodogram, *IEEE Transaction on Audio and Electroacoustics* AU-15 (2) (1967).
- [12] M.C. Vuran, I.F. Akyildiz, Spatial correlation-based collaborative medium access control in wireless sensor networks, *IEEE/ACM Transactions on Networking* 14 (2) (2006) 316–329.
- [13] M. Zuniga, B. Krishnamachari, Analyzing the transitional region in low power wireless links, in: *Proceedings of the IEEE SECON 2004*, October 2004, pp. 517–526.



Baris Atakan received the B.Sc. and M.Sc. degrees in electrical and electronics engineering from Ankara University and Middle East Technical University, Ankara, Turkey, in 2000 and 2005, respectively. He is currently a research assistant in the Next-generation Wireless Communication Laboratory and pursuing his Ph.D degree at the Department of Electrical and Electronics Engineering, Koc University. His current research interests include nano-scale communication, nanonetworks, and biologically-inspired communication protocols for wireless networks.



Ozgur B. Akan received the B.S. and M.S. degrees in electrical and electronics engineering from Bilkent University and Middle East Technical University, Ankara, Turkey, in 1999 and 2001, respectively. He received the Ph.D. degree in electrical and computer engineering from the Broadband and Wireless Networking Laboratory, School of Electrical and Computer Engineering, Georgia Institute of Technology, Atlanta, in 2004. He is currently Associate Professor with the Department of Electrical and Electronics

Engineering, Koc University and the Director of Next-generation Wireless Communications Laboratory (NWCL). His current research interests are in wireless communications, bio-inspired communications, nano-scale and molecular communications, network information theory.

Akan is an Associate Editor for IEEE Transactions on Vehicular Technology, Editor for Nano Communication Networks Journal (Elsevier), ACM/Springer Wireless Networks (WINET) Journal, International Journal of Communication Systems (Wiley). He served as an Area Editor for AD HOC Networks Journal (Elsevier) (between 2004 and 2008), as a Guest Editor for several special issues, as the TPC Co-Chair for ACM MSWiM 2010, General Co-Chair for The Third International Conference on Bio-Inspired Models of Network, Information, and Computing Systems (ICST/IEEE BIONETICS 2008), the European Vice Chair for The Second International Conference on Nano-Networks (ICST/ACM Nano-Net 2007), an International Vice Chair for IEEE INFOCOM 2006, and in organizing committees and technical program committees of many other international conferences. He is the Vice President for IEEE Communications Society – Turkey Section. He is an IEEE Senior Member (Communications Society), and a member of ACM. Dr. Akan received the IBM Faculty Award 2010 and 2008, Turkish Academy of Sciences Distinguished Young Scientist Award 2008 (TUBA-GEBIP).